The divergence of two independent lineages of an endemic Chinese gecko, *Gekko swinhonis*, launched by the Qinling orogenic belt

JIE YAN, QIUXIAN WANG, QING CHANG, XIANG JI and KAIYA ZHOU

Jiangsu Key Laboratory for Biodiversity and Biotechnology, College of Life Sciences, Nanjing Normal University, Nanjing 210046, China

Abstract

The genetic structure and demographic history of an endemic Chinese gecko, *Gekko swinhonis*, were investigated by analysing the mitochondrial cytochrome *b* gene and 10 microsatellite loci for samples collected from 27 localities. Mitochondrial DNA data provided a detailed distribution of two highly divergent evolutionary lineages, between which the average pairwise distance achieved was 0.14. The geographic division of the two lineages coincided with a plate boundary consisting of the Qinling and Taihang Mts, suggesting a historical vicariant pattern. The orogeny of the Qinling Mts, a dispersal and major climatic barrier of the region, may have launched the independent lineage divergence. Both lineages have experienced recent expansion, and the current sympatric localities comprised the region of contact between the lineages. Individual-based phylogenetic analyses of nucDNA and Bayesian-clustering approaches revealed a deep genetic structure analogous to mtDNA. Incongruence between nucDNA and mtDNA at the individual level at localities outside of the contact region can be explained by the different inheritance patterns and male-biased dispersal in this species. High genetic divergence, long-term isolation and ecological adaptation, as well as the morphological differences, suggest the presence of a cryptic species.

Keywords: *Gekko,* lineage divergence, microsatellite DNA, mtDNA, phylogeography, vicariance

Received 11 January 2010; revision received 1 April 2010; accepted 8 April 2010

Introduction

Gekko swinhonis (Reptilia: Gekkonidae) is a gekkonid lizard endemic to China, inhabiting the Loess Plateau, Huabei Plain, Huanghuai Plain, and areas north of the Yangtze River. Previous studies of this species mainly involved morphology (Cai *et al.* 2002), reproductive ecology (Feng *et al.* 2001), breeding behaviour (Jiang *et al.* 1999), isozyme electrophoresis (Shen *et al.* 1996), and phylogeny of the genus *Gekko* or Gekkonidae (Han *et al.* 2001; Zhou & Wang 2008). However, intraspecific differentiation has been discussed in only very few studies. Specimens from Shaanxi province differed from those from other localities in having no distinct or

enlarged tubercles among granular scales (Zhou 1999). Comparative studies on microdermatoglyphic characters also indicated differences between specimens sampled from the northern and southern sides of the Qinling Mts (Liang 1999). The intraspecific differentiation has been attributed to the geographical barriers (Qinling Mts) and the marked ecological differences between these regions (Liang 1999). The Qinling Mts form a natural barrier between northern and southern China, extending along a west–east axis from southeastern Gansu province into Shaanxi and Henan provinces. The Loess Plateau habitat (north of the Qinling Mts) differs from other habitats in its arid climate (annual precipitation < 400 mm), whereas others are characterized by higher humidity and precipitation.

Despite the intraspecific morphological variations, no subspecies have been designated, and until now we

Correspondence: Kaiya Zhou, Fax: 86 25 85891526;
E-mail: kyzhounj@126.com

have had no information on molecular divergence or population structure of this species. Furthermore, the observed morphological variation and habitat differences make this species an interesting model for studies of phylogeography, population dynamics and historical adaptation. In phylogeographical studies which were based on a single mitochondrial gene, phenomena such as homoplasy, independent evolution, incomplete lineage sorting, and biases caused by different modes of inheritance, effective population sizes and sex-biased dispersal can all lead to erroneous results and conclusions (Flanders *et al.* 2009). One way to minimize the impact of such problems is to combine markers with different modes of inheritance and rates of evolution (Hewitt 2004), and therefore recent papers are increasingly making use of multiple markers (such as Leache *et al.* 2009). We applied both maternally inherited mtDNA and bi-parentally inherited microsatellite DNA data in this study. Our primary aims were: (i) to assess the level and partitioning of the genetic variation within *G. swinhonis*; (ii) to analyse the demographic history of populations and events and factors that have influenced it; (iii) to determine the extent of agreement between patterns of genetic variation of different marker types across the whole species range.

Materials and methods

Geographical sampling

Sampling was designed to cover most of the range of *G. swinhonis* across the temperate zones in China. A total of 455 specimens were collected from 27 localities in 2006–2008. Sampling strategies were different for mtDNA and microsatellite DNA. For mtDNA, we sequenced 301 samples from all 27 sites (6–16 samples per site, Table 1). The microsatellite DNA analysis requires large sample sizes, so all individuals collected were examined. Two sequences from congeneric species, *G. auriverrucosus* and *G. japonicus*, were utilized as outgroups for the phylogenetic analyses of the mtDNA. The sampling code and population localities are given in Table 1, and the map of collecting localities is shown in Fig. 1.

Laboratory protocols

Tails were dissected from geckos and stored in 95% ethanol. Voucher specimens are held in the Institute of Genetic Resources, College of Life Sciences, Nanjing Normal University. Genomic DNA was extracted following the standard phenol/chloroform extraction methods. Fragments of complete cytochrome *b* gene (1140 bp) from the mitochondrial genome were targeted

for sequencing with primers L-14731: GAA AAA CTA TCG TTG TTA TTC AAC TA-3′ (Tanaka-Ueno *et al.* 1998), and H-Thr-2: GTT TAC AAG GTC AGC GCT TT-3′ (designed for this study). PCRs were carried out in 50 μL volumes containing 5.0 μL 10 × Buffer, 1.5 mM MgCl$_2$, 0.2 mM each dNTP, 0.2 μM each of primers, 5–10 ng of template DNA and 1.25 U of *Taq* DNA polymerase (TaKaRa Biotechnology, Dalian). The PCR cycling parameters were 95 °C for 4 min, 35 cycles of 95 °C for 40 s, 50 °C for 50 s, 72 °C for 50 s, and one cycle of 72 °C for 10 min. PCR products were then purified and sequenced in both directions by Shanghai Sangon Biological Engineering Technology and Service Co., Ltd. Internal primers (H-cytb-w: GGG ATT TTG TCG GTG CTG GAG TTT-3′ and L-cytb-w: ACA CGC TTC TTT ACC TTC CA-3′) were used in the sequencing amplification. All *G. swinhonis* haplotypes and sequences from two outgroup taxa were deposited in GenBank as accession numbers GQ131337–GQ131373 and GQ857615–GQ857616 (Table 1).

Nuclear DNA of the 455 samples was analysed using the following 10 microsatellite loci: GS103, 104, 111, 112, 119, 123, 133, 210, 223, and 224 (Li & Zhou 2007). The procedure for PCR amplification was similar to that described by Li and Zhou (2007). Fragments were separated on 6.5% polyacrylamide gels and genotyped on an LI-COR DNA Analyser 4300, using the Saga software and controlled with an internal-lane size standard (STR Marker, LI-COR Bioscience).

Mitochondrial DNA analysis

The chromatograms of each sequence were proofread and then assembled using Seqman Pro (DNASTAR). Nucleotide sequences were aligned using MEGA 4 (Tamura *et al.* 2007). No insertions, deletions, or stop codons were present in the alignment. Mean sequence divergences among the major clades were calculated using MEGA 4 and the pairwise Kimura two-parameter (K2P). For phylogenetic analyses, we performed maximum likelihood (ML), maximum parsimony (MP), and Bayesian inference (BI) by using the programs PAUP* 4.0 (Swofford 2002) and MrBayes 3.1.2 (Ronquist & Huelsenbeck 2003). Modeltest 3.7 (Posada & Crandall 1998) and MrModeltest 2.3 (Nylander 2004) were run to determine the appropriate model of molecular evolution in a likelihood ratio test framework based on the Akaike Information Criterion (AIC) for the ML and BI method, respectively. Bootstrap analyses were performed with 1000 replicates for the maximum parsimony method and 100 full heuristic replicates for the maximum likelihood method. For the Bayesian inference, both partitioned (defining each codon position as separate partition) and nonpartitioned analyses were

Table 1 Collection data for *Gekko swinhonis* specimens included in this study

Locality	County, Province (Abbr.)	*n*	Clade	Haplotype no.	Coordinates	GenBank accession no.
1	Huludao, Liaoning (HLD)	12/13	A	1, 4, 26	40°43′N; 120°50′E	GQ131337, 40, 62
2	Shedao, Liaoning (SD)	11/37	A	1, 4	38°57′N; 120°59′E	GQ131337, 40
3	Tianjin (TJ)	10/12	A	1, 24, 32	39°10′N; 117°10′E	GQ131337, 60, 68
4	Baoding, Hebei (BD)	8/10	A	1–3	38°52′N; 115°29′E	GQ131337–39
5	Shijiazhuang, Hebei (SJZ)	12/13	A	1	38°04′N; 114°29′E	GQ131337
6	Hengshui, Hebei (HS)	14/15	A	1, 4–6	37°44′N; 115°41′E	GQ131337, 40–42
7	Wudi, Shandong (WD)	10/12	A	1–2, 25	37°44′N; 117°36′E	GQ131337–38, 61
8	Laixi, Shandong (LX)	9/9	A	1, 26	36°51′N; 120°26′E	GQ131337, 62
9	Laiyang, Shandong (LA)	8/24	A	1, 4	36°57′N; 120°42′E	GQ131337, 40
10	Linyi, Shandong (LI)	7/7	A	1	35°03′N; 118°20′E	GQ131337
11	Zoucheng, Shandong (ZC)	7/9	A	1	35°24′N; 116°58′E	GQ131337
12	Qingxu, Shanxi (QX)	15/22	A, B	33–35	37°34′N; 112°23′E	GQ131369–71
13	Pingding, Shanxi (PD)	6/6	A, B	1, 37	37°42′N; 113°41′E	GQ131337, 73
14	Pinglu, Shanxi (PL)	13/21	B	17, 29	34°50′N; 111°13′E	GQ131353, 65
15	Meixian, Shaanxi (MX)	15/30	B	16–17, 28–31	34°09′N; 107°51′E	GQ131352–53,64–67
16	Lintong, Shaanxi (LT)	14/36	B	16–17, 27	34°29′N; 109°17′E	GQ131352–53, 63
17	Xunyang, Shaanxi (XY)	15/36	A	1, 15	32°50′N; 109°21′E	GQ131337, 51
18	Boai, Henan (BA)	16/16	B	7–11	35°10′N; 113°03′E	GQ131343–47
19	Luoyang, Henan (LY)	6/8	B	9, 12, 16–18	34°39′N; 112°27′E	GQ131345, 48, 52–54
20	Luanchuan, Henan (LC)	14/29	B	12	33°47′N; 111°36′E	GQ131348
21	Shangqiu, Henan (SQ)	11/12	A	1, 4, 13	34°24′N; 115°38′E	GQ131337, 40, 49
22	Nanyang, Henan (NY)	9/10	A	1, 14–15	32°59′N; 112°33′E	GQ131337, 350–51
23	Xuzhou, Jiangsu (XZ)	9/12	A	1, 36	34°16′N; 117°12′E	GQ131337, 72
24	Lianshui, Jiangsu (LS)	19/19	A	1	33°47′N; 119°15′E	GQ131337,
25	Fuyang, Anhui (FY)	11/15	A	19–22	32°55′N; 115°50′E	GQ131355–358
26	Huaiyuan, Anhui (HY)	11/12	A	1, 15, 23–24	33°01′N; 117°02′E	GQ131337, 51, 59–60
27	Zaoyang, Hubei (ZY)	9/10	A	1	32º07′N; 112º46′E	GQ131337
Outgroup						
Gekko auriverrucosus						
Yuncheng, Shanxi (YC)		1	—	—		GQ857615
Gekko japonicus						
Zhoushan, Zhejinag (ZS)		1	—	—		GQ857616

For each population sampled (alphanumeric locality codes refer to those in Fig. 1), we list collection localities (county, province, and exact coordinates), sample sizes subjected to mtDNA/microsatellite DNA examination, the unique mtDNA haplotype numbers, GenBank accession numbers, and the clade (A or B) represented.

performed. Two separate runs including a total of four independent tree searches were conducted. All searches consisted of one 'cold' and three 'heated' Markov chains estimated for 10^6 generations, and every 100 generations were sampled. The burn-in parameter was estimated by plotting $-\ln L$ against the generation number using TRACER v1.4.1 (Rambaut & Drummond 2007), and the retained trees were used to estimate the consensus tree and the Bayesian posterior probabilities. Haplotype network was estimated using median-joining (Bandelt *et al.* 1999) as implemented in NETWORK v 4.5.1.0 (Fluxus Technology, Ltd).

Haplotype diversity, nucleotide diversity (Nei 1987), and Tajima's D (Tajima 1989) were calculated using DnaSP 5.0 (Librado & Rozas 2009). Hierarchical analysis of molecular variance (AMOVA) was performed to compare levels of genetic diversity within and among several possible population groups by using Arlequin v3.11 (Excoffier *et al.* 2005) with 1000 permutations. Those groups maximize values of Φ_{CT} and are statistically significant, indicating the most parsimonious geographical subdivisions. We used Arlequin v3.11 to test the concordance of our cytochrome *b* data with the predicted distribution under a model of sudden expansion (Rogers & Harpending 1992) and measured the smoothness of the mismatch distribution as estimated by the raggedness index.

Recent Bayesian methods (Drummond *et al.* 2005) that make it possible to time major demographic changes such as declines or expansions and to estimate the magnitude and severity of such events (Heller *et al.* 2008) were also used to infer detailed characteristics of demographic history. We applied the Bayesian skyline plot (BSP) model by using the software BEAST v1.5.2
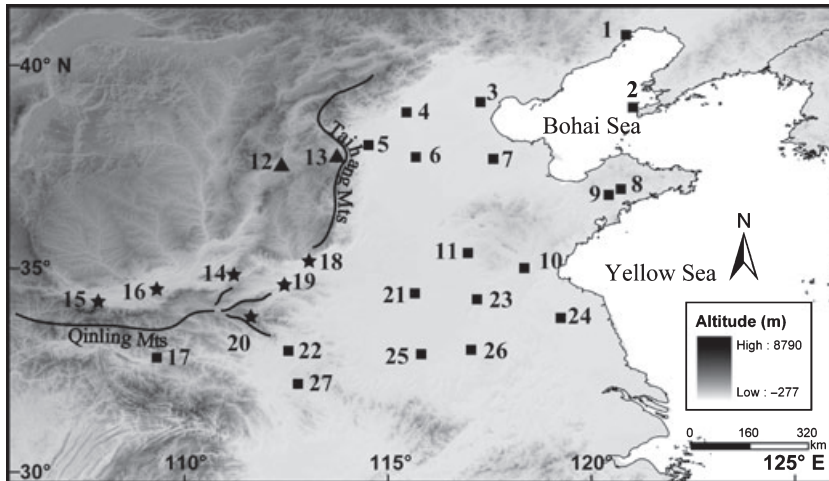
Fig. 1 Sampling sites and mitochondrial haplotype distribution of *G. swinhonis* population. The numbers indicate local populations (see Table 1 for details). The mitochondrial lineages have been labelled by square for lineage A and star for lineage B, respectively. Sympatric sites of both lineages were labelled by triangles.

(Drummond & Rambaut 2007). As a change-point model, BSP allows us to examine a number of different population sizes through time and use a smoothing procedure to visualize historical population size changes. Using this model, it is possible to plot a population size as far back in time as the most recent common ancestor (MRCA) of a set of sequence samples with associated uncertainty. The MCMC chains were run with 10^7 iterations and trees were sampled every 1000 iterations. The first 10% of the iterations were discarded as burn-in. Log files were analysed in TRACER v1.4.1, and effective sample sizes (ESS) were used to evaluate MCMC convergence within chains. A molecular clock ranging from 0.005 to 0.0125 substitutions per site per million years (corresponding to a pairwise genetic distance of 1.0–2.5% per Myr) was used, based on the evolutionary rates of cytochrome *b* estimated in several lizards studies (such as Gübitz *et al.* 2000; Crochet *et al.* 2004; Poulakakis *et al.* 2005). All other parameters within the BSP model were given uniform distributions with wide ranges incorporating all realistic values.

We also used the program BEAST v1.5.2 to estimate the divergence time between the major lineages. For these analyses, we used the model of evolution identified by MrModeltest and a constant coalescent model for the prior estimate of population growth. The MCMC chains were run with 10^7 iterations and trees were sampled every 1000 iterations. The first 10% of the iterations were discarded as burn-in. Under these conditions, the MCMC process performed well, achieving good stationarity and yielding large effective sample size (>200) for estimates of the MRCA. We used a range of sequence divergence rates (1–2.5% per Myr). We conducted nine long runs, three each at fixed mutation rates of 1%, 1.5%, and 2.5%, and from these generated an average MRCA. Our credibility interval included the lower limit from the 1% runs and the upper limit from the 2.5% runs. Hence, this approach yields the most conservation bounds possible under this range of divergence rates.

Microsatellite DNA analysis

All loci were screened for null alleles and large allele dropouts using Micro-Checker v2.2.3 (Van Oosterhout *et al.* 2004). Molecular diversity indices and tests for Hardy–Weinberg equilibrium (HWE) and linkage disequilibrium (LD) were performed in each population as well as a globally unified population using Arlequin v3.11 and Fstat v2.9.3.2 (Goudet 2002).

We analysed the genetic structure of our data set with two different methods. First, we used a phylogenetic tree based on the shared allele distance between individuals and reconstructed using a neighbour-joining algorithm as implemented in the software Populations v1.2.30 (Langella 2007). Second, using a Bayesian approach implemented in Structure v2.3.1 (Hubisz *et al.* 2009), we estimated the number of genetic clusters in the data and assigned the individuals to those different clusters. The admixture model was used and the number of clusters (*K*) was varied from 1 to 27. For each *K*, 10 runs were executed with 10^6 iterations after 10^5 iterations were discarded as 'burn-in'. The most likely number of clusters was estimated using the method of Evanno *et al.* (2005).

Results

Mitochondrial DNA

Of the entire 1140 bp of cytochrome *b* sequences, 222 nucleotides were variable and 216 were parsimony-informative. Thirty-eight, 11 and 173 variable sites were

in the first, second, and third codon positions, respectively. No indels or premature stop codons were observed. This result, together with a strong bias against guanine (mean $G = 13.4\%$, $A = 29.9\%$, $T = 28.7\%$ and $C = 28.0\%$), implied that the target fragment is mitochondrial cytochrome b gene rather than its nuclear homologue. We identified 37 haplotypes among the 301 sequences in *G. swinhonis*. Ten of these were unique haplotypes, 17 were shared within local populations and 10 were shared among local populations. The most abundant haplotype H1, shared by 130 individuals, was widely distributed in 19 local populations (Table 1).

All phylogenetic analyses resulted in almost identical tree topologies, and Fig. 2 shows the nonpartitioned Bayesian tree along with the posterior probabilities and bootstrap values obtained by MP and ML methods. Two major monophyletic haplogroups were revealed in *G. swinhonis*, designated here as clade A and clade B. Clade A occupied most of the range of this species, whereas clade B was mostly restricted to the northern slope of the Qinling Mts. Two local populations located in the west of Taihang Mts possessed haplotypes from both clades (site 12 and 13 in Fig. 1). Clade A can further be subdivided into two subclades: A1 and A2. These two subclades had no geographical specificity, and were admixed in many local populations. The mean pairwise distance between haplotypes in clade A and B, at 0.14, was much higher than that either within clade A (0.026) or clade B (0.012). Within clade A, the mean distance between subclade A1 and A2 was 0.064, also higher than that either within subclade A1 (0.008) or A2 (0.008). With a mutation rate of 1–2.5% per Myr, the average estimate of the MRCA was 17.165 Ma (credibility interval between 12.794 and 18.604 Ma), indicating a Miocene split between lineages.

Diversity indices, h and π, are summarized in Table 2. For the whole samples, h was 0.798 (±0.023) and π was 0.064 (±0.002), indicating a moderate haplotype and high nucleotide diversity. Results of the AMOVA are shown in Table 3. When populations were clustered into two groups, AMOVA gave the highest Φ_{CT} value (0.794, $P < 0.001$). This grouping pattern was concordant with the division of the Qinling Mts and the division of the mtDNA gene tree. The positions of population QX and PD (site 12 and 13), which had
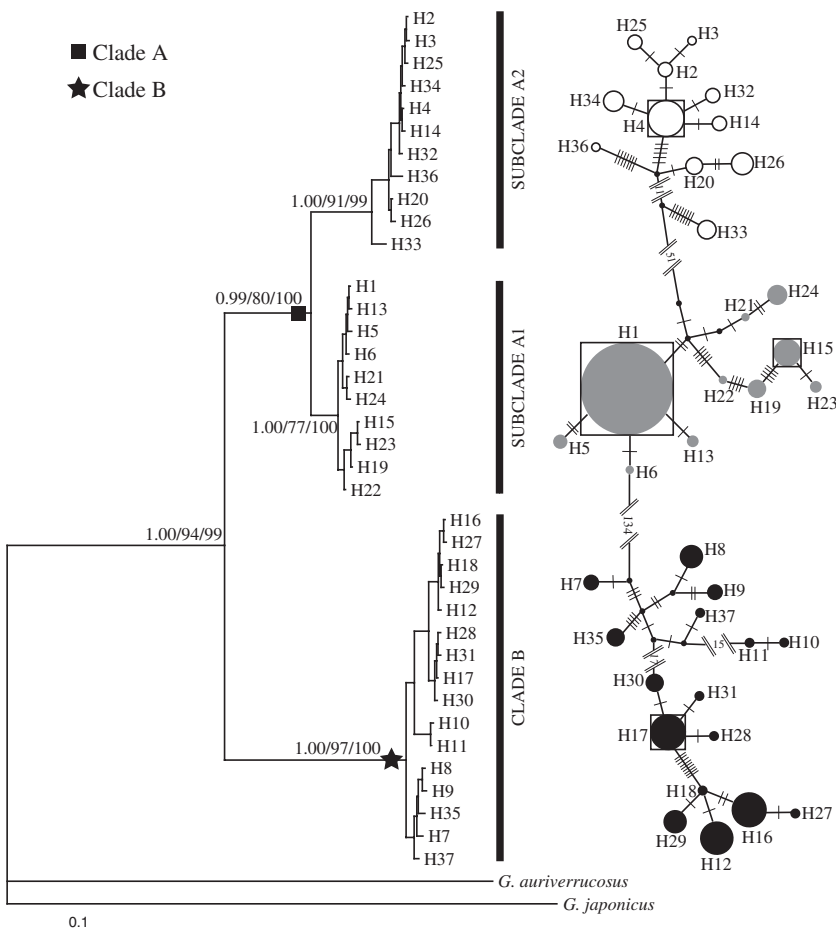

Fig. 2 Phylogenetic trees and the median-joining network based on cytochrome b haplotypes. Numbers above the tree branches are the posterior probabilities, bootstrap values for MP and ML methods. Dashes in network represent the corresponding mutation steps. Haplotypes within a frame are inferred ancestral haplotypes.

Table 2 Genetic diversity and demographic statistics for cytochrome *b* sequences

	n	*N*	*h* ± SD	*π* ± SD	*g* ± SD	*D*	SSD	Raggedness
Clade A	217	21	0.629 ± 0.037	0.025 ± 0.002	38.876 ± 15.191	2.011	0.09962	0.15534
Clade B	84	16	0.887 ± 0.016	0.012 ± 0.001	−49.760 ± 55.770	0.699	0.03664*	0.03767*
Total	301	37	0.798 ± 0.023	0.064 ± 0.002	−2.983 ± 6.346	3.289**	0.06785*	0.06374***

n, number of individuals; *N*, number of haplotypes; *h*, haplotype diversity; *π*, nucleotide diversity; g, population growth parameter; *D*, Tajima's *D* value; SSD, sum of square deviation (goodness-of-fit to a simulated population expansion); Raggedness, raggedness index. (*$P < 0.05$, **$P < 0.01$, ***$P < 0.001$)

Table 3 Results of AMOVA for groupings of *Gekko swinhonis* estimated using Φ-statistics based on cytochrome *b* sequences

	Among groups	Among pops	Within pops	Percentage of variation (%)		
Group compositions†	Φ_{CT}	Φ_{SC}	Φ_{ST}	Among groups	Among pops	Within pops
Two groups						
[1–13, 17, 21–27][14–16, 18–20]	0.794***	0.416***	0.879***	79.39	8.57	12.04
[1–11, 17, 21–27][12–16, 18–20]	0.718***	0.501***	0.859***	71.80	14.13	14.07
Three groups						
[1–11, 13, 17, 21–27][14–16, 18–20] [12]	0.792***	0.358***	0.867***	79.17	7.45	13.37
[1–11, 17, 21– 27][14–16, 18–20][12–13]	0.780***	0.364***	0.860***	78.01	8.02	13.98
Five groups						
[1–9] [12–13][10–11,21, 23–26][14–16, 18–20] [17, 22, 27]	0.706***	0.334***	0.804***	70.63	9.82	19.54
Seven groups						
[1–2][3–7][8–9] [12–13][10–11, 21, 23–24] [14–16, 18–20] [17, 22, 25–27]	0.719***	0.267***	0.794***	71.86	7.52	20.62

pops, populations; ***$P < 0.001$.
†Locality numbers as in Table 1 are enclosed by square brackets.

haplotypes from both clades, was in accordance with the predominant haplotype.

To provide evidence for historical demographic changes, we analysed lineage A, B and the total specimens through neutrality tests, goodness of fit to a simulated population expansion, raggedness index, and growth parameter (Table 2). For lineage A, a signal for demographic expansion was supported by non-significant raggedness index and the mismatch distribution did not deviate significantly from the expected distribution under a sudden expansion model. Positive growth parameter (38.876) also agreed with demographic expansion. For lineage B, negative growth parameter indicated no expansion. However, the significant but low-value raggedness index suggested the opposite. According to the value of τ (15.139), expansion of lineage A took place about 0.53–1.32 Ma.

Results obtained by Bayesian method based on coalescent theory showed detailed demographic histories for both lineages. The two lineages had similar demographic history, and the most prominent feature of the BSPs was a slight decline followed by a sharp increase in effective population size. As shown in Fig. 3, population size of lineage A was relatively stable until approximately 0.36 Ma. Decline was followed by an increase starting at ~0.17 Ma. The demographic change of lineage B was somewhat recent, with a decline at ~0.25 Ma, and soon after an increase at about 0.16 Ma. ESSs were generally high (>300) for all parameters, indicating good MCMC mixing in the combined chains.

Microsatellites

A total of 455 individuals were typed and scored at 10 microsatellite loci. Genetic variation at these loci was very high. The number of alleles per locus ranged from 14 to 35 with a mean of 25.9. The mean observed heterozygosity was 0.6744 and the mean expected heterozygosity was 0.8753. The deficit in observed heterozygosity can be explained by the presence of several distinct populations in our data set.

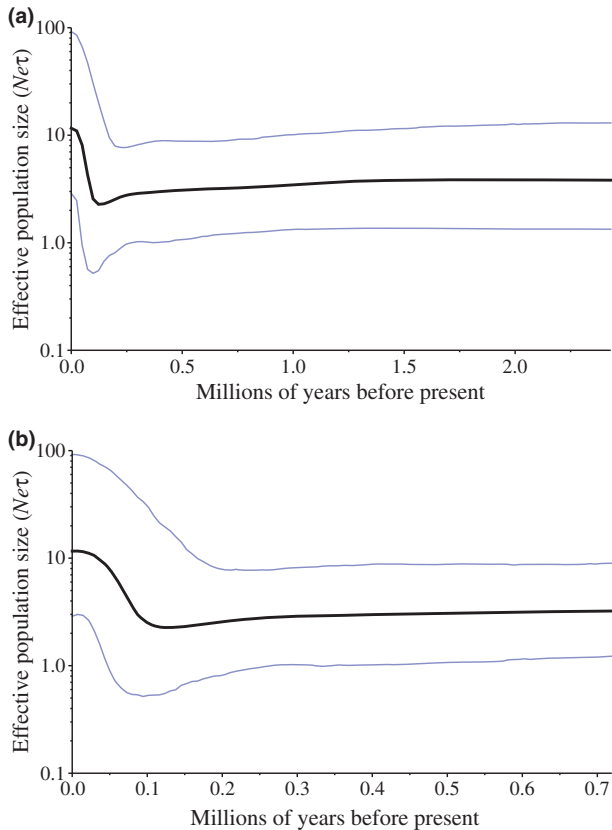Both individual-based analyses of microsatellite data supported the presence of divergent genetic units in the

Fig. 3 Bayesian skyline plots (BSPs). Dark lines represent mean inferred N_E, blue lines mark the 95% highest probability density (HPD) intervals in all panels. (a) For mitochondrial lineage A, and (b) for lineage B.

whole range of this species. Overall, the clustering of individuals in the microsatellite tree based on the shared allele distance was highly congruent with the clustering in the evolutionary lineages (A and B) observed in mtDNA data (Fig. 4). Among the 301 individuals with known mitochondrial lineage attributes, 33 individuals (11%) were assigned to different clusters compared with the mtDNA tree. These individuals were sampled in the regions where the different evolutionary lineages are sympatric (such as in QX and PD, site 12 and 13, respectively), and also unexpectedly in regions far away from the boundaries of two lineages (such as SJZ, TJ, WD, LS, FY, etc.).

Assignment tests using the Bayesian method of structure identified two genetic clusters (K = 2). The Distruct (Rosenberg 2004) diagram showed a strong pattern of genetic structure, broadly consistent with the AMOVA results based on mtDNA data but including some misassignment of individuals, which suggested that individuals clustered differently from the analogous mtDNA lineage (Fig. 5). Recent gene flow between adjacent populations may best explain this misassignment.

Discussion

Qinling orogeny and lineage divergence

Phylogenetic analyses revealed two reciprocally monophyletic lineages in *G. swinhonis*, the lowland lineage (A) and the Qinling lineage (B). As shown in Fig. 1, the Qinling–Taihang Mts seem to act as the boundary between the two lineages. The Qinling Mts create a major mountain chain in Shaanxi province, China. The average altitude of 2000–2800 m has made it a natural boundary between the North and South of the country. The northern side is prone to cold weather, whereas the plains to the south enjoy a sub-tropical climate, with rich, fertile landscape supporting a wealth of wildlife and vegetation. The orogenesis of the Qinling Mts was thought to have begun in the Late Triassic ($\sim$230 Ma) (Zhang *et al.* 1996), and during the Miocene–Pliocene period the mountain was further uplifted to about 1000 m, thus forming a natural barrier separating the South and North (Zhang *et al.* 2004). According to our calculation of the MRCA, we approximately estimated the divergence time between lineages to be 17.165 Ma (95% HPD, 12.794–18.604 Ma). Compared with the geographic record, *G. swinhonis* may have been separated by the Qinling Mts into two lineages, and then the two lineages evolved independently in different circumstances with no interlineage gene flow. Genetic divergence was also evidenced by morphological differences. Specimens sampled from Shaanxi province have been described as having no distinct enlarged tubercles among small granular scales (Zhou 1999), and a previous study on microdermatoglyphics has identified the significant differences in *G. swinhonis* specimens sampled from Xi'an (near to site 16 in Fig. 1) and Xunyang (site 17). The differences have been attributed to the isolation and different ecological factors between the northern and southern slopes of the Qinling Mts (Liang 1999), and we have provided molecular genetic support for the former in this study. Lineage A was further divided into two sublineages, A1 and A2, between which the mitochondrial sequence divergence was 0.0064. Considering that these two sublineages are sympatrically distributed in many local populations, and that there are no evident sign of isolation, we suggest that subclades in the phylogenetic tree can be attributed to the loss of intermediate haplotypes.

Similar effects of mountains on population isolation and lineage divergence have also been reported in other tetrapods. For the tailed frog (*Ascaphus truei*), the major lineage divergence may have possibly emerged during the Late Miocene in response to the rise of the Cascade Mountain range in North America (Nielson *et al.* 2001).

Fig. 4 Unrooted neighbour-joining tree based on microsatellite genotypes of *Gekko swinhonis* individuals. Individuals cluster overall consistently with the mtDNA lineages (Fig. 2), and in analogy, we refer to the nucDNA clusters as nucA and nucB (indicated with open symbols in the periphery). Individuals with affiliated to a different lineage with nucDNA than with mtDNA are marked with small filled symbols of the respective mtDNA lineage. Genotype names are composed of the abbreviation of the location of origin of the specimen.
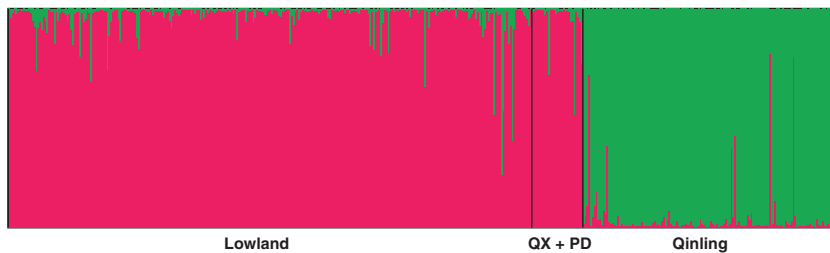
Fig. 5 Bayesian cluster analysis of the microsatellite variation among populations. Each vertical bar represents one individual and its probabilities of being assigned to clusters. Two colours represent two genetic clusters.

In China, the existence of Qinling Mountains and Liu-pan Mountains has been speculated to be one of the causes of lineage divergence of the ring-necked pheasant (*Phasianus colchicus*) occurring in the late Pleistocene (Qu *et al.* 2009). Climatic change along the Helan-Yin mountain chain resulting from sea level rise may have initiated the divergence between two mitochondrial lineages of toad-headed lizards (*Phrynocephalus przewalskii*) (Urquhart *et al.* 2009).

Demographic history

Lineage A was mainly distributed in plain areas north of the Yangtze River. Several undetected or lost intermediate haplotypes, separation of the subclades by as many as 61 mutational steps, and atypical star-like radiation from the 'ancestral' haplotypes (H1 and H4) imply the presence of a bottleneck in the past. H1, the most common haplotype, was discovered in 130 individuals sampled from 19 of the 27 sites, which suggests a recent expansion. Unimodal mismatch distribution, positive growth parameter and nonsignificant raggedness index all support the presence of population expansion for lineage A. This is only a qualitative hypothesis about a historical event, and BSP gives out a more detailed and straightforward output of demographic change within population. In the BSP, lineage A experienced a long-lasting decline and thereafter a rapid expansion. The inferred demographic history of lineage A coincides with its current genetic pattern. From the abscissa (Fig. 3a), we can tell that the expansion event began at about 0.17 Ma, and the trend was slowed down recently. From the value of τ calculated by Arlequin v3.11, another time (0.53–1.32 Ma) since expansion was estimated. Although we cannot identify which time is more exact, the time scale from 0.17 to 1.32 Ma suggests that climate changes in the Pleistocene may have some impact on the demographic changes of lineage A.

The distribution of lineage B was restricted to the northern side of the Qinling Mts. Population size of this lineage also experienced a complex course of decline and increase. Expansion was estimated to occur at about 0.16 Ma close to the time when the lineage A expanded. There are two localities, QX and PD (sites 12 and 13), where haplotypes from both mitochondrial lineages have been found. Excluding H1, which is ancestral (internal node haplotype in network, Fig. 2 right) and widely distributed, all haplotypes are derived (tip haplotypes in network) and have limited distribution. Based on the derived status and restricted distribution of most haplotypes, it appears that the expansion of both lineages has resulted in the current sympatry in locality QX and PD (site 12 and 13), at the west side of

the Taihang Mts. The Taihang Mts were formed during the mountain-building processes of the Jurassic period. They rose steeply from the Huabei Plain to an elevation of approximately 1000–1200 m above sea level. The range stretches some 400 km from north to south, forming the boundary between Shanxi and Hebei provinces, between the Shanxi plateau and the Huabei Plain. Along the whole range, there are eight age-old natural passes breaking the mountains. The fifth pass 'Jingxing' is located in Jingxing county (Hebei province), just between our localities PD and SJZ (sites 13 and 5). Accordingly, individuals of lineage A probably dispersed through the Taihang Mts via this pass and came into secondary contact with lineage B at PD and QX. The limit of sympatric localities is compatible with the idea that the range expansion of an mtDNA lineage may be significantly impeded upon contact with conspecifics. No similar sample sites were located on either side of other seven passes, and possible expansion via these passes could not be detected during this study.

Male-biased dispersal

In this study, mtDNA sequence data revealed a clear vicariant history of *G. swinhonis*. Individual-based analyses of microsatellite data also supported the presence of divergent genetic units in the whole range of this species. The main differences in lineage affiliation between marker types concerned individual geckos from the QX, PD and some other localities such as SJZ, TJ, WD, LS, FY, etc. (Fig. 5). Locality QX and PD have been identified as a secondary contact zone of the two mitochondrial lineages, thus the presence of mixed nuclear clusters was probably a result of hybridization between lineages. However, the incongruence of mtDNA with nucDNA at some other localities can be explained by their different inheritance combined with male-biased dispersal in *G. swinhonis*. Sex-biased gene flow is not unusual in vertebrates, and has been detected for example in red fox (Gachot-Neveu *et al.* 2009); polar bears (Zeyl *et al.* 2009); frogs (Lampert *et al.* 2003); birds (Lecomte *et al.* 2009) and lizards (Johansson *et al.* 2008; Ujvari *et al.* 2008; Urquhart *et al.* 2009). Generally male-biased gene flow in lizards has been associated with polygynous mating systems and female philopatry, and the genetic consequence is that the phylogeographic patterns preserved in mtDNA will be eroded partially and step by step by the gene flow of nucDNA.

Taxonomic consideration

In this study, two divergent evolutionary lineages in *G. swinhonis* have been revealed by analyses of the

mitochondrial cytochrome *b* sequences, with a mean pairwise (K2P) sequence distance up to 0.14 (14%). Although intra- and interspecific molecular divergences in reptile and amphibian species tend to be higher than that in mammals and birds (Johns & Avise 1998), the divergence of 14% is still exceptionally high. Compared with the average genetic distance between congeneric species for reptiles (13.6%) (Harris 2002); wall lizards (genus *Podarcis*) (8.8–17.6%) (Harris & Sa-Sousa 2002); and genus *gekko* (16.7–37.5) (Zhou & Wang 2008), the percentage difference shows us that the sequence divergence level within *G. swinhonis* reached a value more commonly associated with interspecific divergences. Additionally, isolation of more than 10 Myr and adaptation to different environmental factors can provide a favourable environment for speciation. In fact, morphological differences have also been found in *G. swinhonis*. All together, this information suggests that the two divergent lineages probably are independent lineages. However, compared with the general definitions of three different categories of candidate species (Vieites *et al.* 2009), this speculation may be confused by the genetic admixture of the two lineages at sympatric sites. In addition, sympatric occurrence with admixture may be caused by introgressive hybridization between closely related species, which has been documented in a variety of animal species (Weisrock *et al.* 2005; Maroja *et al.* 2009). Further studies including morphology, ecology, development, behaviour, etc. are required to resolve this issue.

Acknowledgements

References

Bandelt HJ, Forster P, Rohl A (1999) Median-joining networks for inferring intraspecific phylogenies. *Molecular Biology and Evolution*, **16**, 37–48.

Cai Y, Xu J, Lu W *et al.* (2002) Histology of hemipenis of *Gekko swinhonis*. *Chinese Journal of Anatomy*, **25**, 489–492.

Crochet PA, Chaline O, Surget-Groba Y, Debain C, Cheylan M (2004) Speciation in mountains: phylogeography and phylogeny of the rock lizards genus *Iberolacerta* (Reptilia: Lacertidae). *Molecular Phylogenetics and Evolution*, **30**, 860–866.

Drummond AJ, Rambaut A (2007) BEAST: Bayesian evolutionary analysis by sampling trees. *BMC Evolutionary Biology*, **7**, 214.

Drummond AJ, Rambaut A, Shapiro B, Pybus OG (2005) Bayesian coalescent inference of past population dynamics from molecular sequences. *Molecular Biology and Evolution*, **22**, 1185–1192.

Evanno G, Regnaut S, Goudet J (2005) Detecting the number of clusters of individuals using the software STRUCTURE: a simulation study. *Molecular Ecology*, **14**, 2611–2620.

Excoffier L, Laval G, Schneider S (2005) Arlequin (version 3.0): An integrated software package for population genetics data analysis. *Evolutionary Bioinformatics*, **1**, 47–50.

Feng Z, Li Z, Zhang C (2001) Studies on reproductive ecology and biology of the *Gekko swinhonis*. *Zoological Research*, **22**, 83–84.

Flanders J, Jones G, Benda P *et al.* (2009) Phylogeography of the greater horseshoe bat, *Rhinolophus ferrumequinum*: contrasting results from mitochondrial and microsatellite data. *Molecular Ecology*, **18**, 306–318.

Gachot-Neveu H, Lefevre P, Roeder JJ, Henry C, Poulle ML (2009) Genetic detection of sex-biased and age-biased dispersal in a population of wild carnivore, the red fox, *Vulpes vulpes*. *Zoological Science*, **26**, 145–152.

Goudet J (2002) Fstat, a program to estimate and test gene diversities and fixation indices (version 2.9.3.2). Available from http://www2.unil.ch/popgen/softwares/fstat.htm.

Gübitz T, Thorpe RS, Malhotra A (2000) Phylogeography and natural selection in the Tenerife gecko *Tarentola delalandii*: testing historical and adaptive hypotheses. *Molecular Ecology*, **9**, 1213–1221.

Han D, Zhou K, Wang Y (2001) Phylogeny of ten species of Chinese gekkonid lizards (Gekkonidae: Lacertilia) inferred from 12S rRNA sequences. *Acta Zoologica Sinica*, **47**, 139–144.

Harris DJ (2002) Reassessment of comparative genetic distance in reptiles from the mitochondrial cytochrome *b* gene. *Herpetological Journal*, **12**, 85–86.

Harris DJ, Sa-Sousa P (2002) Molecular phylogenetics of Iberian wall lizards (*Podarcis*): is *Podarcis hispanica* a species complex? *Molecular Phylogenetics and Evolution*, **23**, 75–81.

Heller R, Lorenzen ED, Okello JB, Masembe C, Siegismund HR (2008) Mid-Holocene decline in African buffalos inferred from Bayesian coalescent-based analyses of microsatellites and mitochondrial DNA. *Molecular Ecology*, **17**, 4845–4858.

Hewitt GM (2004) Genetic consequences of climatic oscillations in the Quaternary. *Philosophical Transactions of the Royal Society of London. Series B, Biological Sciences*, **359**, 183–195.

Hubisz MJ, Falush D, Stephens M, Pritchard JK (2009) Inferring weak population structure with the assistance of sample group information. *Molecular Ecology Resources*, **9**, 1322–1332.

Jiang Y, Wu W, Tian M, Zhao S (1999) The breeding habits of *Gekko swinhonis*. *Sichuan Journal of Zoology*, **18**, 114–116.

Johansson H, Surget-Groba Y, Thorpe RS (2008) Microsatellite data show evidence for male-biased dispersal in the Caribbean lizard *Anolis roquet*. *Molecular Ecology*, **17**, 4425–4432.

Johns GC, Avise JC (1998) A comparative summary of genetic distances in the vertebrates from the mitochondrial cytochrome *b* gene. *Molecular Biology and Evolution*, **15**, 1481–1490.

Lampert KP, Rand AS, Mueller UG, Ryan MJ (2003) Fine-scale genetic pattern and evidence for sex-biased dispersal in the

tungara frog, *Physalaemus pustulosus. Molecular Ecology*, **12**, 3325–3334.

Langella O (2007) Populations 1.2.30: population genetic software, individuals or populations distances, phylogenetic trees. Available from http://bioinformatics.org/~tryphon/populations/.

Leache AD, Koo MS, Spencer CL *et al.* (2009) Quantifying ecological, morphological, and genetic variation to delimit species in the coast horned lizard species complex (*Phrynosoma*). *Proceedings of the National Academy of Sciences, USA*, **106**, 12418–12423.

Lecomte N, Gauthier G, Giroux JF, Milot E, Bernatchez L (2009) Tug of war between continental gene flow and rearing site philopatry in a migratory bird: the sex-biased dispersal paradigm reconsidered. *Molecular Ecology*, **18**, 593–602.

Li JJ, Zhou KY (2007) Isolation and characterization of microsatellite markers in the gecko *Gekko swinhonis* and cross-species amplification in other gekkonid species. *Molecular Ecology Notes*, **7**, 674–677.

Liang G (1999) Comparative study on the microdermatoglyphics of four species of *Gekko. Zoological Research*, **20**, 67–70.

Librado P, Rozas J (2009) DnaSP v5: a software for comprehensive analysis of DNA polymorphism data. *Bioinformatics*, **25**, 1451–1452.

Maroja LS, Andres JA, Harrison RG (2009) Genealogical discordance and patterns of introgression and selection across a cricket hybrid zone. *Evolution*, **63**, 2999–3015.

Nei M (1987) *Molecular Evolutionary Genetics*. Columbia University Press, New York.

Nielson M, Lohman K, Sullivan J (2001) Phylogeography of the tailed frog (*Ascaphus truei*): implications for the biogeography of the Pacific Northwest. *Evolution*, **55**, 147–160.

Nylander JAA (2004) *MrModeltest v2. Program distributed by the author*. Evolutionary Biology Centre, Uppsala University.

Posada D, Crandall KA (1998) MODELTEST: testing the model of DNA substitution. *Bioinformatics*, **14**, 817–818.

Poulakakis N, Lymberakis P, Valakos E *et al.* (2005) Phylogeography of Balkan wall lizard (*Podarcis taurica*) and its relatives inferred from mitochondrial DNA sequences. *Molecular Ecology*, **14**, 2433–2443.

Qu JY, Liu NF, Bao XK, Wang XL (2009) Phylogeography of the ring-necked pheasant (*Phasianus colchicus*) in China. *Molecular Phylogenetics and Evolution*, **52**, 125–132.

Rambaut A, Drummond AJ (2007) Tracer v1.4. Available from http://beast.bio.ed.ac.uk/Tracer.

Rogers AR, Harpending H (1992) Population growth makes waves in the distribution of pairwise genetic differences. *Molecular Biology and Evolution*, **9**, 552–569.

Ronquist F, Huelsenbeck JP (2003) MrBayes 3: Bayesian phylogenetic inference under mixed models. *Bioinformatics*, **19**, 1572–1574.

Rosenberg NA (2004) DISTRUCT: a program for the graphical display of population structure. *Molecular Ecology Notes*, **4**, 137–138.

Shen J, Lu P, Chen Y (1996) The comparative study on LDH isozymes of six tissues of three species of *Gekko. Journal of Nanjing Normal University (Natural Science)*, **19**, 45–47.

Swofford DL (2002) *PAUP*—Phylogenetic Analysis Using Parsimony (* and Other Methods. Beta version 4.0b10)*. Sinauer Associates, Sunderland.

Tajima F (1989) Statistical method for testing the neutral mutation hypothesis by DNA polymorphism. *Genetics*, **123**, 585–595.

Tamura K, Dudley J, Nei M, Kumar S (2007) MEGA4: Molecular Evolutionary Genetics Analysis (MEGA) software version 4.0. *Molecular Biology and Evolution*, **24**, 1596–1599.

Tanaka-Ueno T, Matsui M, Chen SL, Takenaka O, Ota H (1998) Phylogenetic relationships of brown frogs from Taiwan and Japan assessed by mitochondrial cytochrome *b* gene sequences (Rana: Ranidae). *Zoological Science*, **15**, 283–288.

Ujvari B, Dowton M, Madsen T (2008) Population genetic structure, gene flow and sex-biased dispersal in frillneck lizards (*Chlamydosaurus kingii*). *Molecular Ecology*, **17**, 3557–3564.

Urquhart J, Wang Y, Fu J (2009) Historical vicariance and male-mediated gene flow in the toad-headed lizards *Phrynocephalus przewalskii. Molecular Ecology*, **18**, 3714–3729.

Van Oosterhout C, Hutchinson WF, Wills DPM, Shipley P (2004) MICRO-CHECKER: software for identifying and correcting genotyping errors in microsatellite data. *Molecular Ecology Notes*, **4**, 535–538.

Vieites DR, Wollenberg KC, Andreone F *et al.* (2009) Vast underestimation of Madagascar's biodiversity evidenced by an integrative amphibian inventory. *Proceedings of the National Academy of Sciences, USA*, **106**, 8267–8272.

Weisrock DW, Kozak KH, Larson A (2005) Phylogeographic analysis of mitochondrial gene flow and introgression in the salamander, *Plethodon shermani. Molecular Ecology*, **14**, 1457–1472.

Zeyl E, Aars J, Ehrich D, Wiig O (2009) Families in space: relatedness in the Barents Sea population of polar bears (*Ursus maritimus*). *Molecular Ecology*, **18**, 735–749.

Zhang G, Meng Q, Yu Z *et al.* (1996) Orogenesis and dynamics of the Qinling orogen. *Science in China (Series D)*, **39**, 225–234.

Zhang Y, Qu Y, Wu S, He F, Shi J (2004) The research introduction of engineering geology in Qinling orogenic belt. *Journal of Engineering Geology*, **12**, 44–49.

Zhou K (1999) Genus *Gekko*. In:*Fauna Sinica, Reptilia Vol. 2, Squamata, Lacertili* (eds Zhao E-m, Zhao K, Zhou K). pp. 31–53, Science Press, Beijing.

Zhou K, Wang Q (2008) New species of *Gekko* (Squamata: Sauria: Gekkonidae) from China: morphological and molecular evidence. *Zootaxa*, **1778**, 59–68.

J. Yan is a molecular phylogeneticist whose interests include phylogeny and phylogeography of amphibians and reptiles. Q. Wang teaches biology at Hohhot Second Middle School. She was a graduate student at Nanjing Normal University where she explored population genetics and cryptic diversity in geckos. Q. Chang is a vertebrate researcher whose interests include wildlife management in airports, and molecular phylogeography of birds and mammals. X. Ji is a reptile evolutionary ecologist mainly focusing on geographic patterns and genetic correlations of life history reaction norms in reptiles. K. Zhou is a vertebrate biologist whose interests include conservation biology, molecular phylogeny and molecular phylogeography.